Stress Relaxation and Inverse Stress Relaxation in Silk Fibers

V. K. KOTHARI, R. RAJKHOWA, V. B. GUPTA

Department of Textile Technology, Indian Institute of Technology, Hauz Khas, New Delhi 110016, India

Received 10 July 1999; accepted 7 April 2000

ABSTRACT: Stress-relaxation experiments on four varieties of Indian silk fiber show that stress relaxation is significantly greater in non-Mulberry silks than in the Mulberry silk and that the differences among non-Mulberry silk fibers are relatively small. All the fibers studied also exhibit inverse stress relaxation. It has been shown that the Maxwell–Wiechert model, with two Maxwell elements in parallel, can be used to analyze and explain both the stress-relaxation and inverse stress-relaxation behaviors.
 J Appl Polym Sci 82: 1147–1154, 2001

Key words: silk fiber; stress relaxation; inverse stress relaxation; Maxwell–Wiechert model; Mulberry silk; Muga silk; Tasar silk; Eri silk

INTRODUCTION

The load-elongation and recovery behavior of the four Indian silk fibers[1,2] show considerable differences, which arise mainly from the differences in their structures.[1,3] Compared to the non-Mulberry silk fibers, Mulberry silk fiber has crystallites of smaller size, higher molecular orientation, and a more compact overall packing of molecules.[1,3] Stress-relaxation studies, which provide another route to study time dependence shown by fibers and thus gain an understanding of their viscoelastic behavior, were carried out and are reported in this communication. During the course of these studies, it was observed that the silk fibers also show the phenomenon of "inverse relaxation," which has been investigated for textile fibers,[4] including silk fibers.[5] To gain some understanding of the inverse relaxation phenomenon, the results were analyzed using the Maxwell–Wiechert model[6] based on two Maxwell elements in parallel.

Correspondence to: V. K. Kothari.

Journal of Applied Polymer Science, Vol. 82, 1147–1154 (2001)

EXPERIMENTAL

Materials

Sufficient quantities of crossbreed bivoltine and multivoltine Mulberry, temperate Tasar (bivoltine), Muga (multivoltine), and Eri (multivoltine) cocoons were collected from different sources in northeast India for the investigation. Mulberry, Eri, and Muga silk samples were obtained from Assam (India), and Tasar silk sample was obtained from Manipur (India).

Methods

Processing of Cocoons

Mulberry cocoons were cooked in plain water at 90–95°C for about 15 min. Tasar and Muga cocoons were cooked in water containing 0.5 wt % sodium carbonate with material-to-liquor (MLR) ratio of 1 : 20 for 20 min at 95°C. Temperate Tasar cocoons were cooked using 0.5% sodium carbonate and 0.5% sodium silicate at 90°C for 30 min. Eri cocoons, which are open mouthed, were not reelable, so no cooking was done for Eri cocoons. The cooked cocoons were brushed manually to obtain filament ends.

In the case of Eri silk, cocoons were degummed in a water bath (MLR = 1 : 20) containing 5% sodium carbonate and 1% nonionic wetting agent for 3 h at 95°C. Five layers from outside to inside of the cocoon were then separated.

Reeling

Each cocoon was reeled out using a laboratory wrap reel. While reeling, successive reeled lengths of 30 m were cut and numbered sequentially so as to identify location of these small filament segments in a cocoon during subsequent testing. Care was taken during the reeling to ensure that the filament was not stretched and properties did not change during reeling. The temperature and other conditions of reeling of different silk fibers were as follows:

Mulberry	Distilled water at 40–45°C.
Muga	Na_2CO_3 (0.25%) in distilled water at 40–45°C.
Tasar	Dry reeling after cocoons were lightly pressed to remove water, while allowing them to remain moist.

After reeling, filaments were washed in distilled water to remove any residual alkali present.

Degumming of Reeled-Out Filaments

A number of reeled filaments from different cocoons of the same variety were segregated depending on fineness. Filaments were then degummed separately in groups. Degumming was carried out in small beakers placed in a Julaba, in which beakers swing in a heated water bath. The conditions of degumming were as follows:

Temperature	90°C
Time	3 h
MLR	1 : 50
Additives	Sodium carbonate (2 g/L) + sodium silicate (2 g/L) + nonionic wetting agent (0.25 g/L)

The degummed samples were then treated in the following solvents in the given order to remove any residual fats:

- 8 h in methanol and diethylene ether (3 : 1)
- 24 h in cyclohexane
- 8 h in benzene

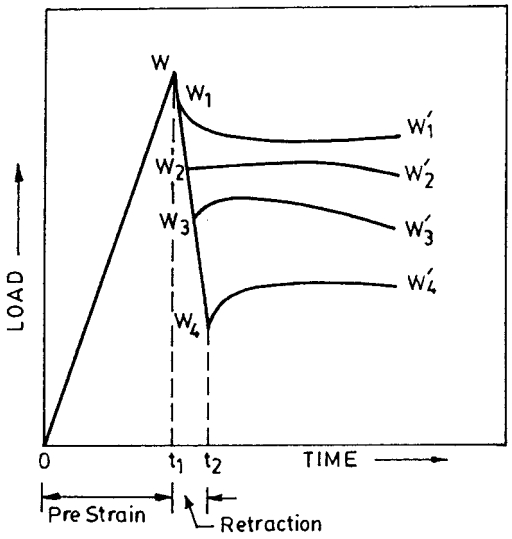

Figure 1 Schematic representation of inverse stress relaxation.

Stress Relaxation

Silk fibers used in stress-relaxation experiments were mechanically conditioned at 2% strain in an Instron Tensile Tester (Model 1112). The samples were subjected to cyclic loading and unloading until reproducible hysteresis loops were obtained. Conditioned fibers of 50-mm gauge length were mounted on paper windows with a pretension of 0.02 gf/den. They were then extended to a fixed strain of 1% and held in that position. The stress in the fiber was recorded as a function of time on a moving chart paper for approximately 20 min. The stress was seen to relax at a rapid rate in the beginning and, with increasing time, the rate of stress relaxation gradually decreased. By the time the experiment was terminated, the stress had become almost constant. Ten samples of each variety were subjected to the stress-relaxation test and the average percentage stress relaxation at different times could be estimated from the curves obtained.

Inverse Stress Relaxation

The silk fibers used in this study were mechanically conditioned as in the case of stress-relaxation experiment. Conditioned fiber of 50-mm gauge length was then extended to a fixed strain of 1% in the case of all samples, except Eri silk, which was subjected to a prestrain of between 1 to 10% at a strain rate of 20%/min. As shown in Figure 1, the application of the initial prestrain

Table I Percentage Stress Relaxation of Silk Fibers at 1000 s After Application of 1% Prestrain

Variety of Silk Fiber	Percentage Stress Relaxed
Mulberry	24.1
Muga	35.5
Tasar	38.4
Eri	42.4

takes a finite time t_1 and results in a load W in the fiber. However, it is generally assumed in stress-relaxation studies that the prestrain is applied in zero time.

Inverse relaxation is known to occur only when the initial prestrain is reduced and the time dependence of stress in the fiber is recorded immediately after reaching the reduced strain level. Therefore, once the jaw had reached its maximum displacement as the fiber was prestrained, it was immediately brought back to a level so that material strain was reduced. The recorded stress then follows different paths with time, depending on the level of retraction of strain, as shown in Figure 1. The following trends are worth noting:

- The load continues to decrease with time and then ultimately becomes almost constant.
- The load does not change initially with time and then decreases slowly.
- Initially the load increases and then slowly decreases with time.
- The load increases with time and then becomes almost constant.

The duration of the experiment was so selected that within the experimental time, the load became almost constant without any further change; in most cases this happened in approximately 10 min. Experiments were conducted for different retraction levels, and the prestrain was reduced to correspond to the reduction of load from between 0 to 100% of the peak load. The ratio $[(W_i - W_i')/W_i] \times 100$, where W_i and W_i' represent load as indicated in Figure 1 (in which i has values 1, 2, 3, and 4), was taken as a measure of relaxation index n. A negative ratio indicates an increase in stress value, whereas a positive value corresponds to stress relaxation. The point at which the transition occurs from negative to positive value will correspond to zero stress relaxation index.

After locating the transition point, experiments were performed at near the transition point to clearly observe the zero relaxation behavior.

RESULTS AND DISCUSSION

Stress Relaxation

The percentage stress relaxation data for the silk fibers (which were taken to a prestrain of 1%, after which the stress in the sample was recorded for 1000 s) are presented in Table I, which clearly shows that stress relaxation is significantly greater in non-Mulberry silks than in the Mulberry silk. Given that stress relaxation is a characteristic of viscoelastic materials, it may be concluded that Mulberry silk fiber is less viscoelastic than the non-Mulberry silk fibers.

It would be expected that these significant differences shown by the silk fibers in their viscoelastic behavior would be related to the difference in their structures. Some relevant structural data taken from another publication[3] is presented in Table II. It is noteworthy that the density, crystalline index, and birefringence of mulberry silk are the highest among the silk fibers studied. This suggests that Mulberry silk fiber has more compact packing of molecules and a higher degree of molecular orientation compared to those of non-Mulberry silk fibers. These characteristics are known to render a fiber closer to an elastic material than to a viscoelastic material.

Analysis of the Data in Terms of the Maxwell–Wiechert Model

Macroscopic phenomenological models[6] comprising mass less Hookean springs and Newtonian dashpots have been widely used to represent lin-

Table II Density, Infrared Crystalline Index, and Birefringence Data for Four Varieties of Silk Fibers

Variety of Silk Fiber	Density (g/cm^3)	Infrared Crystalline Index	Birefringence (Δn)
Mulberry	1.355	0.66	0.052
Muga	1.308	0.50	0.040
Tasar	1.310	0.50	0.040
Eri	1.314	0.60	0.037

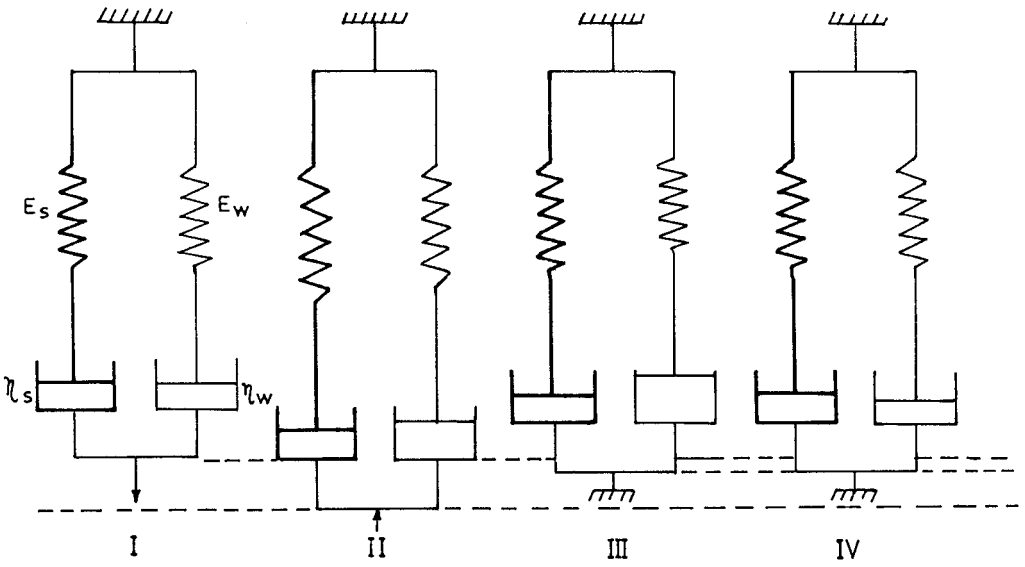

Figure 2 Four-element model at different stages in an inverse stress-relaxation experiment: (I) Start of prestrain; (II) start of retraction, weak dashpot has opened; (III) held at a reduced strain level, weak dashpot is still open and weak spring had been compressed; (IV) inverse stress relaxation, compressed spring releases compression by closing the weak dashpot.

ear viscoelastic behavior. Wilding and Ward[7] discussed the applicability of three such models to creep behavior of ultrahigh modulus polyethylene. They concluded that the creep behavior is best described by the Maxwell–Wiechert model in which two activated processes are coupled in parallel. In this study an attempt was made at simulating the stress-relaxation behavior of silk using the Maxwell–Wiechert model (Fig. 2). This model has two Maxwell elements in parallel. One arm (the left arm in Fig. 2, Stage I) has a strong spring with elastic constant E_s in series with a strong dashpot with viscosity coefficient η_s, and the other arm (the right arm in Fig. 2, Stage I) has a weak spring (E_w) in series with a weak dashpot (η_w). The response of the model to a fixed strain and later to a reduced strain is shown schematically in Figure 2.

When the Maxwell–Wiechert model is subjected to a prestrain of ϵ_0, the stress relaxation starts immediately thereafter and at any time t, the stress $\sigma(t)$ is given by[6]

$$\sigma(t) = E_s\varepsilon_0 e^{-t/\tau_s} + E_w\varepsilon_0 e^{-t/\tau_w} \qquad (1)$$

where $\tau_s = \eta_s/E_s$ and $\tau_w = \eta_w/E_w$ are relaxation times.

The four constants of this model (i.e., E_s, η_s, E_w, and η_w) for a given material were estimated from the experimental data on the stress $\sigma(t)$, as a function of time t, obtained during the stress-relaxation experiment. Equation (1) and the values of $\sigma(t)$ for different values of t in the experimental curve were used to obtain the values of the four constants of the model that gives the minimum least square error. The spring and dashpot constants estimated for the four varieties of silk are presented in Table III. Also indicated in the table are the relaxation times of both the strong and the weak arms of the model.

The calculated values of $\sigma(t)$ as a function of time (t) using the model constants given in Table III for the four varieties of silk are compared with experimental results in Figure 3; the agreement between the theory and experiment is seen to be quite good. Another interesting observation was that, although the strong arm carried most of the load, it was in the weak arm that most of the stress relaxation occurred. This is obvious from the data presented in Figure 4, in which the stresses in the two arms of the model for the four silk fibers are plotted as a function of time.

Inverse Stress Relaxation

The phenomenon of inverse stress relaxation can also be analyzed with the help of the model represented by Figure 2, Stage I, provided it is assumed that during the time taken for prestrain-

Table III Spring Constants, Viscosity Coefficients, and Relaxation Times for Different Varieties of Silk

Variety of Silk Fiber	E_s (GPa)	E_w (GPa)	η_s (GPa/s)	η_w (GPa/s)	$\tau_s = \eta_s/E_s$ (s)	$\tau_w = \eta_w/E_w$ (s)
Mulberry	13.2	3.29	248,338	48.7	18,813.5	14.8
Muga	8.48	3.62	102,973	60.8	13,143.0	15.9
Tasar	5.28	3.3	150,680	121.4	28,537.9	36.8
Eri	4.52	1.75	16,954	15.1	3750.9	8.6

ing the sample at the start of the experiment, the weak dashpot is able to respond to the stress taken up by the weak arm, which, as shown in Table III, has a relatively much lower relaxation time. Further support for this assumption came from a simple experiment on Mulberry silk that was subjected to the same prestrain, first at 20%/min and then at 100%/min. The percentage drop of peak stress for zero relaxation increased from 64% at the lower strain rate to 84% at the higher strain rate. This supports the assumption made and further indicates that, if the time taken for prestraining is negligibly small, there would be no inverse stress relaxation. This can be tested if the instrument is capable of being operated at very high strain rates. The response of the model to various steps leading to an inverse stress relaxation is illustrated in Figure 2, Stages I– IV.

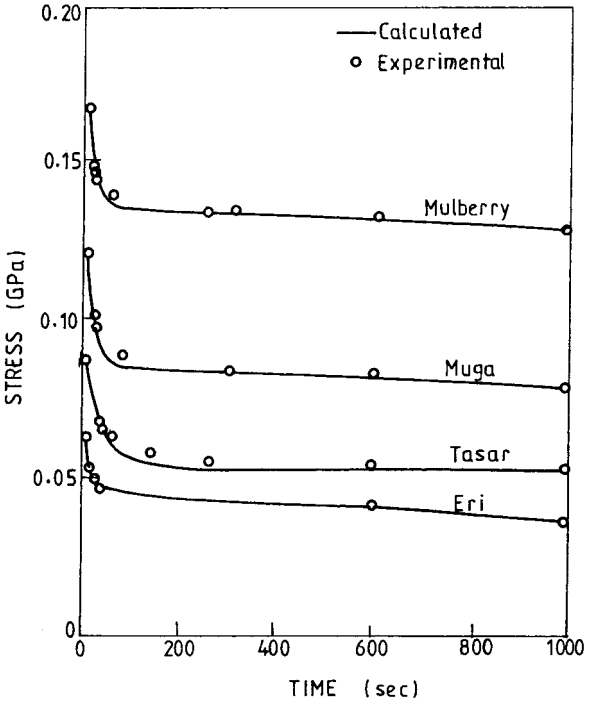

Figure 3 Stress relaxation of silk fibers.

With the assumption that stress in both the strong arm and the weak arm has reduced to an extent depending on the opening of the two dashpots in the course of application of the prestrain, eq. (1) may be modified as follows:

$$\sigma(t) = E_s\varepsilon_{os}e^{-t/\tau_s} + E_w\varepsilon_{ow}e^{-t/\tau_w} \quad (2)$$

where ϵ_{os} is extension of the strong spring ($\epsilon_{os} \leq \epsilon_0$) and ϵ_{ow} is extension of the weak spring ($\epsilon_{ow} < \epsilon_0$).

If the stress is suddenly reduced from its peak value by reducing the strain from ϵ_0 to ($\epsilon_0 - \epsilon_n$), eq. (2) may be written as

$$\sigma(t) = E_s(\varepsilon_{os} - \varepsilon_n)e^{-t/\tau_s} + E_w(\varepsilon_{ow} - \varepsilon_n)e^{-t/\tau_w} \quad (3)$$

where ϵ_n represents the reduction of strain during the inverse relaxation experiment.

It may be noted that ($\epsilon_{ow} - \epsilon_n$) may become negative, depending on the value of ϵ_n. In that situation, a compressive stress develops in the spring. With the passage of time, this stress is dissipated in the weak dashpot as the weak spring opens. Thus, there is an increase in stress from a negative value to zero. This increase in stress may be more than the decrease in stress in the strong arm because the stress reduction in the strong arm is very slow as a result of the presence of the strong dashpot. Thus, the total stress increases in the system. However, once the stress in the weak arm becomes zero or if the reduction in stress of the strong arm becomes greater than the stress increase in the weak arm, the inverse relaxation stops and stress decay starts again. This ultimate reduction of stress may not always be observed during the experimental time because the process is very slow.

The data on percentage drop of peak stress for getting zero stress relaxation for the four differ-

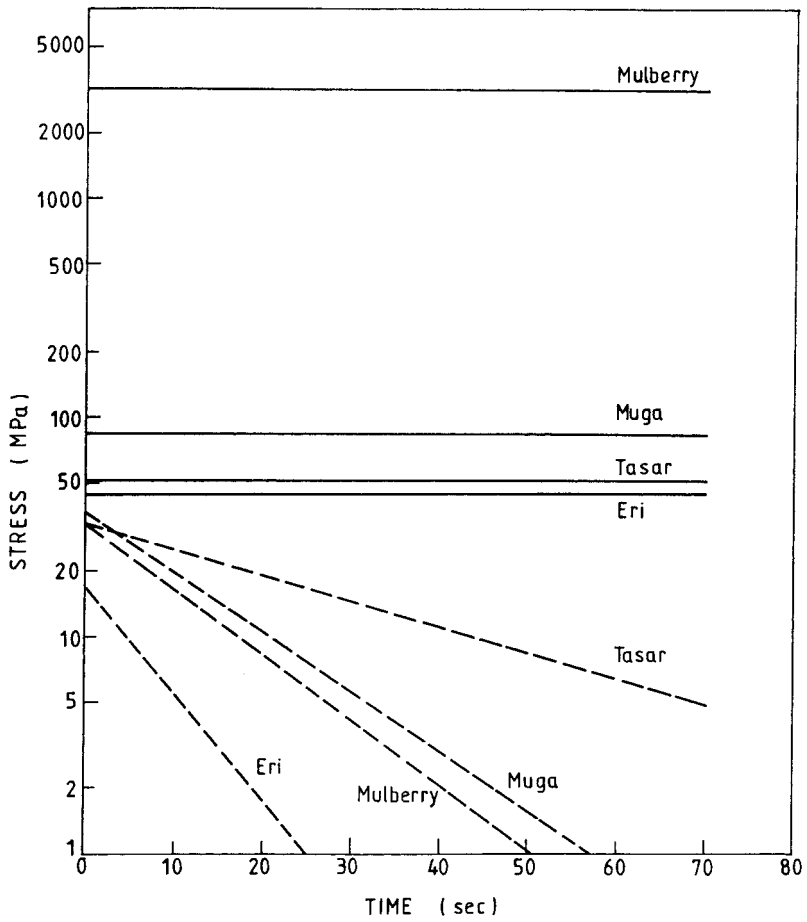

Figure 4 Stress relaxation in strong and weak arms of the model for different silk fibers (—strong arm; – – – weak arm).

ent varieties of silk are given in Table IV. It is interesting to observe that the drop in percentage peak stress to reach the transition from stress relaxation to inverse stress relaxation in case of non-Mulberry silk fibers is lower than that for Mulberry silk fiber.

Table IV Percentage Drop of Peak Stress for Zero Relaxation for Various Silk Fibers

Type of Silk	Percentage Drop of Peak Stress for Getting Zero Relaxation[a]
Mulberry (1.14 den)	64.0[b]
Eri (2.23 den)	58.0
Tasar (2.9 den)	50.0
Muga (3.24 den)	52.0

[a] Prestrain rate: 20%/min.
[b] 84.0 if rate of prestrain is 100%/min.

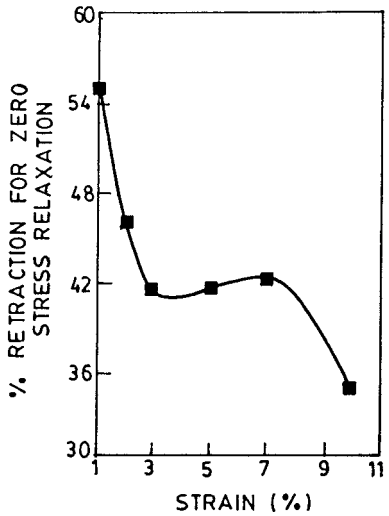

Figure 5 Zero relaxation index as a function of prestrain for Eri silk fiber.

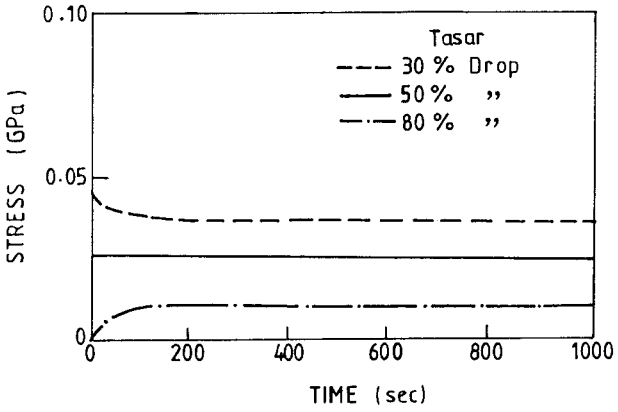

Figure 6 Stress-relaxation and inverse stress-relaxation curves obtained from the model for Tasar silk fiber.

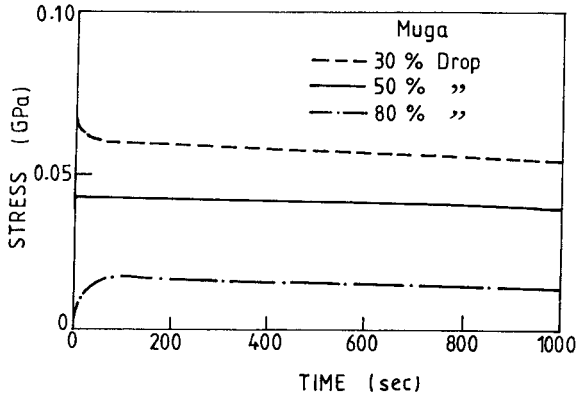

Figure 8 Stress-relaxation and inverse stress-relaxation curves obtained from the model for Muga silk fiber.

The percentage drop of peak stress for getting transition point as a function of strain for Eri silk is shown in Figure 5. As the strain increases, the inverse relaxation commences with a lesser percentage drop in peak stress. However, when the peak load does not change with the increase in strain (3 to 7% strain), the percentage retraction remains almost the same for getting zero stress relaxation index.

The plots corresponding to eq. (3) for given values of ϵ_n (0.003, 0.005, and 0.008) and spring and dashpot constants already worked out, for assumed values of $\epsilon_{ow} = 0.005$ and $\epsilon_{os} = 0.01$ for Tasar silk fiber, are shown in Figure 6.

Figure 7 shows the calculated curve for Tasar silk fiber, in which the increase of stress followed by decrease can be observed when the stress scale is enlarged. This is similar to the experimental observation, particularly when the speed of the Instron chart is increased for a retraction slightly more than the transition point.

Figures 8, 9, and 10 for Muga, Eri, and Mulberry silk fibers, respectively, show the general nature of this phenomenon, which is similar to that shown schematically in Figure 1. Thus this analysis, based on the Maxwell–Wiechert model, suggests that the origin of inverse relaxation is in the viscoelasticity of the sample. The decrease in prestrain, according to the model described in this study, can result in compression of some struc-

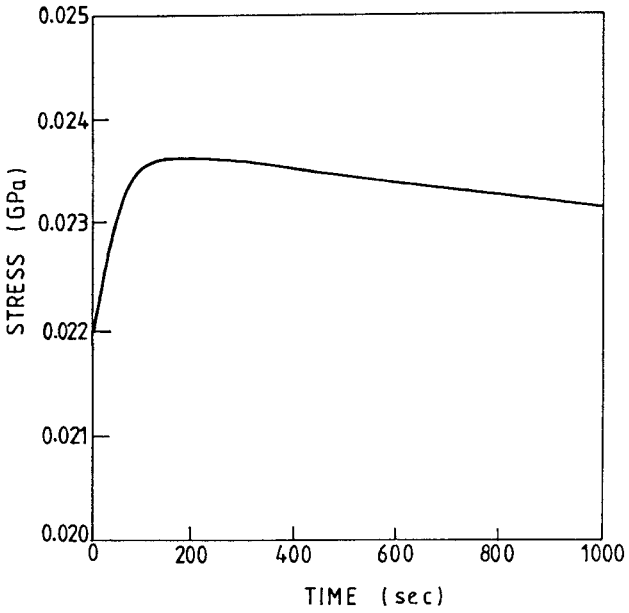

Figure 7 Inverse stress relaxation followed by stress relaxation obtained from the model for Tasar silk fiber.

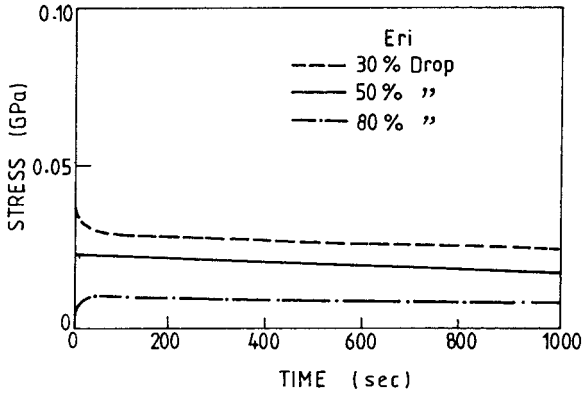

Figure 9 Stress-relaxation and inverse stress-relaxation curves obtained from the model for Eri silk fiber.

tural elements of the fiber. As a consequence, the stress can increase from a negative value to zero, thus giving rise to inverse stress relaxation.

Relaxation Index

The relaxation index n, as obtained for Eri silk fiber, which was studied over a wide range of prestrain, is shown in Figure 11. It is interesting to note that n can vary over a wide range.

CONCLUSIONS

This study has confirmed the following observations:

1. Stress relaxation proceeds at a faster rate in non-Mulberry silk fibers than in Mulberry silk. This observation is consistent with the structural[3] and stress–strain[1] data on this fiber presented elsewhere.
2. Both stress relaxation and inverse stress relaxation of silk fibers are quite adequately represented by the Maxwell–Wiechert model, which comprises two Maxwell elements in parallel.

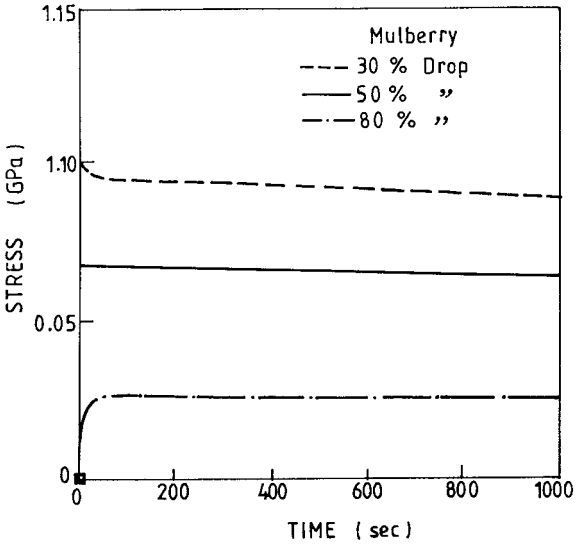

Figure 10 Stress-relaxation and inverse stress-relaxation curves obtained from the model for Mulberry silk fiber.

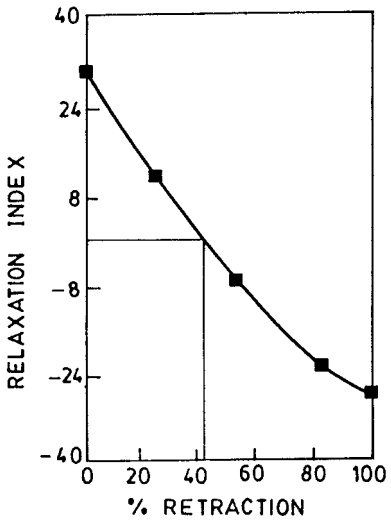

Figure 11 Relaxation index as a function of percentage retraction at 7% prestrain for Eri silk fiber.

REFERENCES

1. Rajkhowa, R.; Gupta, V. B.; Kothari, V. K. J Appl Polym Sci 2000, 77, 2418.
2. Sonwalkar, T. N.; Roy, S.; Vasumathi, B. V.; Hariraj, G. Indian J Sericulture 1989, XXVIII, 159.
3. Gupta, V. B.; Rajkhowa, R.; Kothari, V. K. Indian J Fiber Text Res 2000, 25, 14.
4. Nachane, R. P.; Sundaram, V. J Text Inst 1995, 86, 20.
5. Das, S. Ph.D. Thesis, Indian Institute of Technology, Delhi, 1996
6. Fried, J. R. Polymer Science and Technology; Prentice Hall: Englewood Cliffs, NJ, 1995; pp. 196–205.
7. Wilding, M. A.; Ward, I. M. Plast Rubber Proc Appl 1981, 1, 167.